

Unprecedented Reactivities of Highly Reactive Manganese(III)–Iodosylarene Porphyrins in Oxidation Reactions

Lina Zhang, Yong-Min Lee, Mian Guo, Shunichi Fukuzumi, and Wonwoo Nam*

Cite This: <https://dx.doi.org/10.1021/jacs.0c10159>

Read Online

ACCESS |



Metrics & More



Article Recommendations



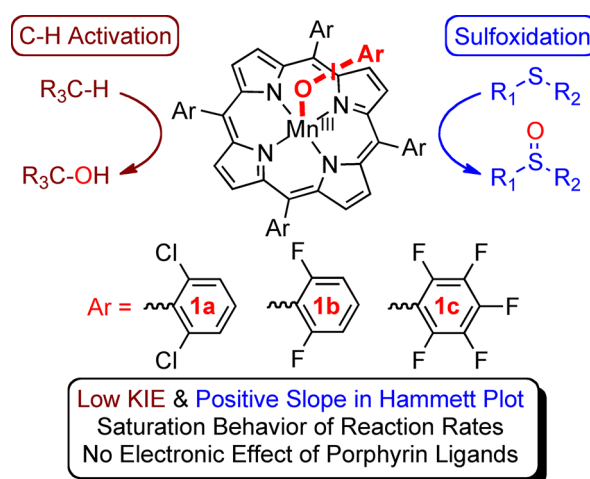
Supporting Information

ABSTRACT: We report that Mn(III)-iodosylarene porphyrins, $[\text{Mn}^{\text{III}}(\text{Porp})(^s\text{ArIO})]^+$, are capable of activating the C–H bonds of hydrocarbons, including unactivated alkanes such as cyclohexane, with unprecedented reactivities, such as a low kinetic isotope effect, a saturation behavior of reaction rates, and no electronic effect of porphyrin ligands on the reactivities of $[\text{Mn}^{\text{III}}(\text{Porp})(^s\text{ArIO})]^+$. In oxygen atom transfer (OAT) reactions, the sulfoxidation of *para*-X-substituted thioanisoles by $[\text{Mn}^{\text{III}}(\text{Porp})(^s\text{ArIO})]^+$ affords a very unusual behavior in the Hammett plot with the saturation behavior of reaction rates and no electronic effect of porphyrin ligands on reactivities. The reactivities and mechanisms of $[\text{Mn}^{\text{III}}(\text{Porp})(^s\text{ArIO})]^+$ are then compared with those of the corresponding $\text{Mn}^{\text{IV}}(\text{Porp})(\text{O})$ complex. The present study reports the first example of highly reactive Mn(III)–iodosylarene porphyrins with unprecedented reactivities in C–H bond activation and OAT reactions.

Heme and nonheme iron enzymes utilize various metal–oxygen intermediates, such as metal-oxo, -superoxo, -peroxo, and -hydroperoxo species, in the oxidation of organic compounds.^{1–4} To understand the geometric and electronic structures and the reactivities of the intermediates, reactions of model compounds with artificial oxidants have been extensively investigated over the past several decades.^{1,2,4} Among the artificial oxidants, iodosylarenes (ArIO)⁵ have been frequently used as terminal oxidants in generating metal-oxo intermediates as well as in catalytic oxidation reactions.^{1,2,4} Indeed, a number of metal–oxo complexes have been synthesized using the ArIO oxidant.^{1,2,4,6} In the catalytic oxidation reactions, in addition to the metal-oxo intermediates, metal–iodosylarene adducts ($\text{M}^{\text{n+}}\text{–ArIO}$), which are the precursors of the metal–oxo species, have been proposed as active oxidants that effect the oxidation reactions (i.e., one oxidant versus multiple oxidants debate).⁷ Indeed, $\text{M}^{\text{n+}}\text{–ArIO}$ intermediates have been isolated and characterized spectroscopically and/or structurally.^{8–10} However, those $\text{M}^{\text{n+}}\text{–ArIO}$ complexes were not strong oxidants except a nonheme iron(III)–iodosylarene complex;^{10c} therefore, only a limited number of oxidation reactions were investigated with the isolated $\text{M}^{\text{n+}}\text{–ArIO}$ complexes.^{9,10}

Very recently, we reported the synthesis, characterization, and reactivity of Mn(III)–iodosylarene porphyrins, such as $[\text{Mn}^{\text{III}}(^s\text{ArIO})(\text{TDCPP})]^+$ (**1a**)¹¹ (see Scheme 1 for structure); this intermediate showed high chemo- and stereoselectivity in olefin epoxidation reactions.⁸ In the present study, we demonstrate that **1a** is highly reactive in the C–H bond activation of hydrocarbons and oxygen atom transfer (OAT) reactions (Scheme 1); it is notable that the reactivity of **1a** is comparable to that of the corresponding Mn(IV)–oxo porphyrin complex, $\text{Mn}^{\text{IV}}(\text{O})(\text{TDCPP})$ (**2a**), which is a highly reactive oxidant that effects the C–H bond activation via an oxygen non-rebound mechanism.¹² Interestingly, the Mn(III)–iodosylarene adducts have shown unexpected reactivities

Scheme 1. Mn(III)–Iodosylarene Porphyrins and Their Reactivities in C–H Bond Activation and Sulfoxidation Reactions



in the C–H bond activation and OAT reactions (see Scheme 1). The mechanisms of the oxidation reactions by $[\text{Mn}^{\text{III}}(\text{Porp})(\text{ArIO})]^+$ are also discussed in this study.

The Mn(III)–iodosylarene porphyrins, such as **1a**, $[\text{Mn}^{\text{III}}(^s\text{PhIO})(\text{TDFPP})]^+$ (**1b**),¹¹ and $[\text{Mn}^{\text{III}}(^s\text{PhIO})(\text{TPFPP})]^+$ (**1c**)¹¹ (see Scheme 1 for structures), were synthesized according to the published procedures (Support-

Received: September 23, 2020



ing Information, Experimental Section).⁸ The reactivity of **1a** was then investigated in the C–H bond activation of hydrocarbons. Upon addition of xanthene to **1a** in CH₂Cl₂ at –60 °C, the peak at 462 nm due to **1a** disappeared with the increase of the peak at 477 nm due to [Mn^{III}(TDCPP)]⁺ (Figure 1a). The first-order rate constants increased with

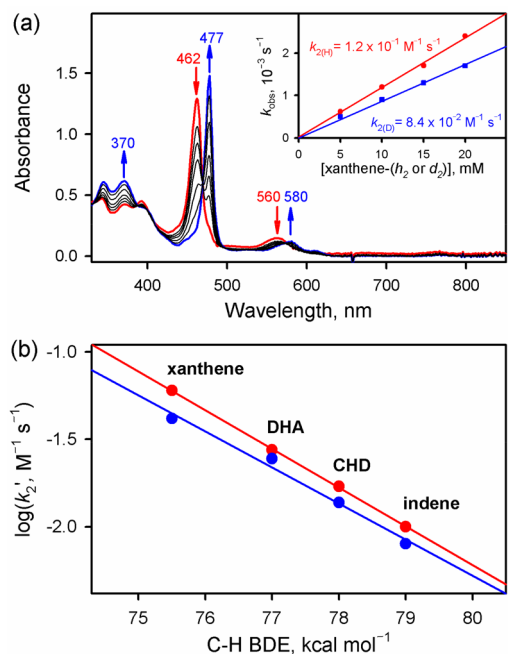


Figure 1. (a) UV–vis spectral changes showing the reaction of **1a** (0.10 mM, red line) and xanthene (15 mM) in CH₂Cl₂ at –60 °C. Inset shows the plots of k_{obs} against concentrations of xanthene (red circles) and xanthene-*d*₂ (blue squares) to determine k_2 values with **1a**. (b) Plots of $\log(k_2')$ ($k_2' = k_2/\text{number of equivalent target C–H bonds}$) against the substrates C–H BDEs for **1a** (red circles) and **2a** (blue circles).

increasing xanthene concentration, giving a second-order rate constant of $1.2 \times 10^{-1} \text{ M}^{-1} \text{ s}^{-1}$ at –60 °C (Figure 1a, inset). Similarly, a second-order rate constant of $8.4 \times 10^{-2} \text{ M}^{-1} \text{ s}^{-1}$ at –60 °C was determined with deuterated xanthene (xanthene-*d*₂) (Figure 1a, inset), giving a KIE value of 1.4. In contrast, a KIE value of 11 was determined in the oxidation of xanthene and xanthene-*d*₂ by a Mn(IV)–oxo complex bearing the same TDCPP ligand (**2a**) (Figure S1). Other Mn(III)–iodosylarene porphyrins also afforded small KIE values in the oxidation of xanthene and xanthene-*d*₂, such as 2.0 for **1b** and 1.4 for **1c** (Figure S2).

When the C–H bond activation by **1a** and **2a** was investigated with other substrates, such as 9,10-dihydroanthracene (DHA, BDE = 77 kcal mol^{–1}),¹³ 1,4-cyclohexadiene (CHD, BDE = 78 kcal mol^{–1}),¹³ and indene (BDE = 79 kcal mol^{–1})¹³ (Table S1 and Figures S3 and S4), good linear correlations between the bond dissociation energies (BDEs) of the substrates and the reaction rate constants were observed (Figure 1b). Interestingly, the reactivity of **1a** was slightly greater than that of **2a** (Figure 1b). In the reactions of DHA, CHD, and indene with other Mn(III)–iodosylarene porphyrins, such as **1b** and **1c**, good linear correlations between the BDEs of the substrates and the reaction rate constants were also observed with similar reactivities (Table S1 and Figures S5–S7), indicating that there is no significant porphyrin ligand

effect on the reactivities of Mn(III)–iodosylarene porphyrins. This observation is of interest because the reactivities of iron-oxo porphyrins are significantly affected by the electronic nature of porphyrin ligands in oxidation reactions, suggesting that the active intermediate may be different from the metal-oxo porphyrin species (*vide infra*).¹⁴

More interestingly, when the C–H bond activation of hydrocarbons, such as xanthene, DHA, CHD, indene, and xanthene-*d*₂, by **1a** was performed with large amounts of substrates, saturation plots were obtained (Figure 2a; Table S2

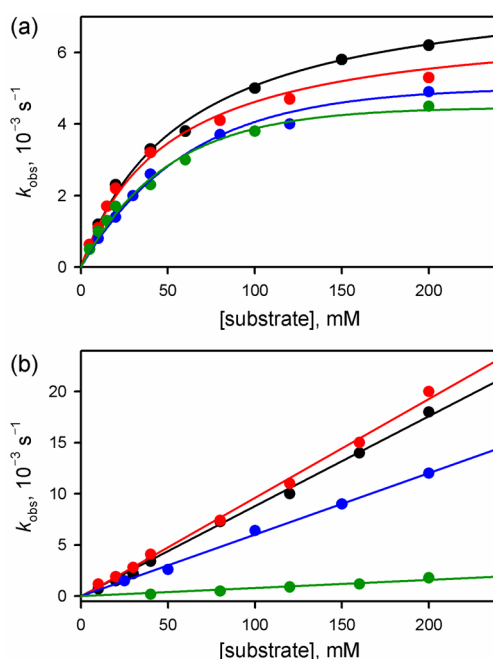
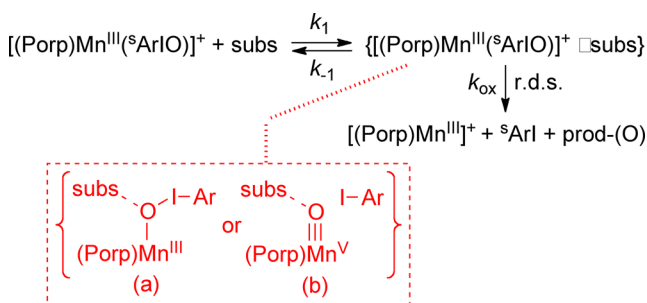


Figure 2. Plots of k_{obs} against concentrations of substrates [xanthene (black circles), DHA (red circles), CHD (blue circles), and xanthene-*d*₂ (green circles)] in the reactions of (a) **1a** and (b) **2a** in CH₂Cl₂ at –60 °C.

and Figure S8). In contrast, a linear correlation between the reaction rates and the substrate concentrations was observed in the reactions of **2a** with the substrates (Figure 2b); the observation of the good linear correlation plot irrespective of the concentration of substrates indicates that a hydrogen atom (H atom) abstraction by **2a** is the rate-determining step (r.d.s.). In contrast, the saturation plots observed in the C–H bond activation reactions by **1a** indicate the presence of a relatively fast equilibrium that precedes the r.d.s. H atom abstraction (Scheme 2) (*vide infra*), as proposed in the C–H bond activation by a Mn(IV)–(oxo)(hydroxo) complex by Costas and co-workers; the latter complex also afforded a low KIE of 2.0 in the C–H bond activation of xanthene.¹⁵

Other substrates with stronger C–H bonds, such as ethylbenzene (BDE = 87 kcal mol^{–1}),¹³ cyclooctane (BDE = 95.7 kcal mol^{–1}),¹³ and cyclohexane (BDE = 99.5 kcal mol^{–1}),¹³ were also oxidized by **1a** (Figure S9). By analyzing products formed in the reactions of Mn(III)–iodosylarene porphyrins and ethylbenzene in CH₂Cl₂ at –60 °C, we found that 1-phenylethanol (78(4)%) was yielded as the oxygenated product (Table S3). In addition, the product(s) formed in the oxidation of cyclohexane by **1a** was cyclohexanol (61(4)%). These results are contrary to the previously reported oxidation of hydrocarbons by Mn(IV)–oxo porphyrins, in which

Scheme 2. Proposed Mechanism for the Oxidation of Substrates by Mn(III)–Iodosylarene Porphyrins



halogenated products were yielded predominantly in halogenated solvents, such as CH_2Cl_2 (Table S3).¹² Further, we found out that oxygen atoms in the oxygenated products formed in the oxidation of ethylbenzene and cyclohexane by ^{18}O -labeled Mn(III)–iodosylarene porphyrins derived from the Mn(III)–iodosylarene porphyrins (Figures S10 and S11). Mn(III) porphyrins were the decay product of Mn(III)–iodosylarene porphyrins (Figure S12).

For the OAT reactions by Mn(III)–iodosylarene porphyrins, we investigated the oxidation of *para*-X-substituted thioanisoles and then compared their reactivities to that of a Mn(IV)–oxo porphyrin complex. First, as observed in the C–H bond activation reactions, saturation plots were obtained when large amounts of substrates were used in the reactions of **1a**, **1b**, and **1c** (Tables S4–S6 and Figures S13–S15), indicating a relatively fast equilibrium that precedes the oxygen transfer to the thioanisole substrates (Scheme 2) (*vide infra*). In contrast, a linear correlation plot was obtained in the oxidation of thioanisoles by **2a** (Figure S16). Second, Hammett plots of Mn(III)–iodosylarene porphyrins and Mn(IV)–oxo porphyrin were compared in the oxidation of *para*-X-substituted thioanisoles using small amounts of substrates (i.e., with initial rates) (Figures S17–S19). Interestingly, positive ρ values were obtained in the oxidation of *para*-X-substituted thioanisoles by Mn(III)–iodosylarene porphyrins when initial rates were plotted against the σ_p^+ of the substrates (Figure 3a, black line and Figure S20, black lines). This observation is contrary to the known fact that electrophilic oxidants exhibit a negative slope in Hammett plot;¹⁶ we attribute the observed positive ρ value to the existence of an equilibrium to form a precursor complex that precedes the OAT to the thioanisole derivatives (Scheme 2) (*vide infra*). It should be also noted that negative ρ values were obtained in the Hammett plot when reaction rates determined with high substrate concentrations were plotted against the σ_p^+ of the substrates (Figure 3a, red line and Figure S20, red lines). In the case of Mn(IV)–oxo porphyrin, a negative ρ value was obtained in the oxidation of thioanisole derivatives by **2a** irrespective of the concentrations of substrates (Figure 3b; Figure S16). Product analysis revealed that $[\text{Mn}^{\text{III}}(\text{TDCPP})]^+$ was formed as the decay product of **1a** (Figure S21) and methyl phenyl sulfoxide (>95%) as the organic product (Figure S22). Finally, we observed no significant porphyrin ligand effect in the oxidation of thioanisoles by Mn(III)–iodosylarene porphyrins (Table S7 and Figures S13–S15), as observed in the C–H bond activation reactions (*vide supra*).

Then, how do we interpret the saturation behavior of reaction rates observed in the C–H bond activation and OAT reactions by Mn(III)–iodosylarene porphyrins? As shown in

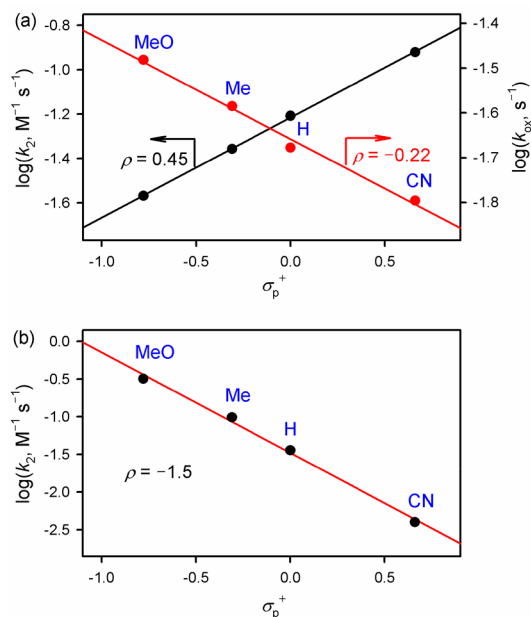


Figure 3. (a) Hammett plots of $\log k_2$ (black circles, a low substrate concentration) and $\log k_{\text{ox}}$ (red circles, a large substrate concentration) against the σ_p^+ values of *para*-X-substituted thioanisoles for the sulfoxidation of thioanisole derivatives by **1a**. (b) Hammett plots of $\log k_2$ against the σ_p^+ values of *para*-X-substituted thioanisoles for the sulfoxidation of thioanisole derivatives by **2a**.

Scheme 2, there is an equilibrium between the Mn(III)–iodosylarene porphyrin and the substrate before the oxidation reaction takes place. Accordingly, the saturation plot can be fitted by eq 1,

$$k_{\text{obs}} = k_{\text{ox}}K_f[\text{subs}]/(1 + K_f[\text{subs}]) \quad (1)$$

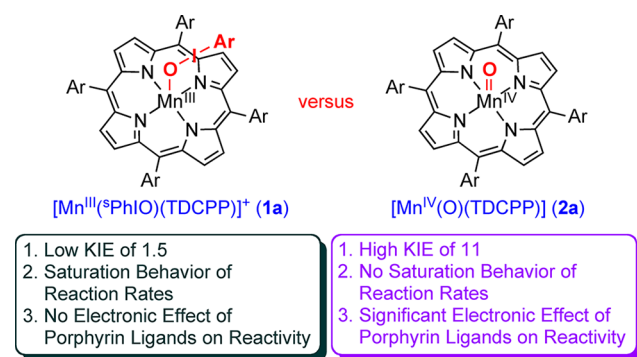
where K_f , which is k_1/k_{-1} , is the formation constant of $\{[(\text{Porp})\text{Mn}^{\text{III}}(\text{sArIO})]^+ \cdot \text{subs}\}^{\ddagger}$ and k_{ox} is the rate constant of the oxidation by $\{[(\text{Porp})\text{Mn}^{\text{III}}(\text{sArIO})]^+ \cdot \text{subs}\}^{\ddagger}$.^{15,17,18} Thus, at high concentrations of substrate (i.e., $K_f[\text{subs}] \gg 1$), k_{obs} becomes k_{ox} , and the existence of $\{[(\text{Porp})\text{Mn}^{\text{III}}(\text{sArIO})]^+ \cdot \text{subs}\}^{\ddagger}$ can explain the independency of the substrate concentration on the reaction rate, such as $k_{\text{obs}} = k_{\text{ox}}$ when $K_f[\text{subs}] \gg 1$.

With invoking the formation of $\{[(\text{Porp})\text{Mn}^{\text{III}}(\text{sArIO})]^+ \cdot \text{subs}\}^{\ddagger}$ between Mn(III)–iodosylarene porphyrins and substrates before the oxidation reaction takes place (Scheme 2), we rationalize the observed positive ρ values in Hammett plots as follows: the formation constant of $\{[(\text{Porp})\text{Mn}^{\text{III}}(\text{sArIO})]^+ \cdot \text{subs}\}^{\ddagger}$, K_f , depends on the electronic interaction between Mn(III)–iodosylarene porphyrins and substrates. That is, the most electron-withdrawing substituent (e.g., *para*-CN-thioanisole) would afford the largest K_f whereas the most electron-donating substituent (e.g., *para*-MeO-thioanisole) would afford the smallest K_f . Therefore, since the k_{ox} values depend on the amount of $\{[(\text{Porp})\text{Mn}^{\text{III}}(\text{sArIO})]^+ \cdot \text{subs}\}^{\ddagger}$ generated, the reaction of the intermediate species with *para*-CN-thioanisole would occur faster than that with *para*-MeO-thioanisole, which resulted in giving a positive ρ value in the reactions performed with small amounts of substrates (Figure 3a, black line and Figure S20, black lines).

Finally, what is the nature of the active oxidant that oxidizes substrates in the oxidation reactions by Mn(III)–iodosylarene porphyrins? Recently, Wang and co-workers proposed two

resonance valence-bond electronic structures from density functional theory (DFT) calculations in an iron(III)–iodosylarene complex-mediated sulfoxidation reaction.¹⁹ Similarly, we propose here that in the cage, such as $[(\text{Porp})\text{Mn}^{\text{III}}(\text{sArIO})]^+\cdot\text{subs}^\ddagger$ in Scheme 2, $[(\text{Porp})\text{Mn}^{\text{III}}(\text{ArIO})]^+$ can oxidize substrate directly (Scheme 2, structure a). Alternatively, $[(\text{Porp})\text{Mn}^{\text{V}}(\text{O})]^+$, which is formed via the O–I bond cleavage of $[(\text{Porp})\text{Mn}^{\text{III}}(\text{ArIO})]^+$, oxidizes substrates (Scheme 2, structure b). Since it has been known that Mn^{V} –oxo complexes of porphyrin and nonporphyrin ligands with a low-spin state ($S = 0$) are sluggish oxidants,²⁰ we may exclude a low-spin $S = 0$ $[(\text{Porp})\text{Mn}^{\text{V}}(\text{O})]^+$ complex as an active oxidant.²¹ Further, reactivities of the $\text{Mn}(\text{III})$ –iodosylarene porphyrins obtained in this study, such as a low KIE (e.g., ~ 1.5) and no porphyrin ligand effect, are very different from those of $\text{Mn}(\text{IV})$ –oxo porphyrins, such as a large KIE (e.g., >10) and a significant porphyrin ligand effect on reaction rates (see Scheme 3). Based on the results

Scheme 3. Reactivity Comparison of $\text{Mn}(\text{III})$ –Iodosylarene Porphyrin versus $\text{Mn}(\text{IV})$ –Oxo Porphyrin Intermediates



discussed above, we propose that $[(\text{Porp})\text{Mn}^{\text{III}}(\text{ArIO})]^+$ is the active oxidant that oxidizes substrates with the unprecedented reactivities presented in this study.

In conclusion, we have reported for the first time that $\text{Mn}(\text{III})$ –iodosylarene porphyrins are highly reactive in the C–H bond activation of hydrocarbons, yielding alcohol products selectively. We have also shown that the reactivities of Mn –iodosylarene porphyrins are very different from those of Mn –oxo porphyrins in the C–H bond activation and sulfoxidation reactions. Thus, the present study demonstrates how diverse the reactivities of metal–oxygen intermediates can be in oxidation reactions. Our future studies will be focused on understanding the chemical properties and reaction mechanisms of metal–iodosylarene complexes in detail as well as the involvement of the highly reactive metal–iodosylarene intermediates in catalytic oxidation reactions.

■ ASSOCIATED CONTENT

Supporting Information

The Supporting Information is available free of charge at <https://pubs.acs.org/doi/10.1021/jacs.0c10159>.

Experimental Section, Tables S1–S7 and Figures S1–S22 (PDF)

■ AUTHOR INFORMATION

Corresponding Author

Wonwoo Nam – Department of Chemistry and Nano Science, Ewha Womans University, Seoul 03760, Korea; School of Chemistry and Chemical Engineering, University of Jinan, Jinan 250022, China; orcid.org/0000-0001-8592-4867; Email: wnnam@ewha.ac.kr

Authors

Lina Zhang – Department of Chemistry and Nano Science, Ewha Womans University, Seoul 03760, Korea;

orcid.org/0000-0003-4539-2741

Yong-Min Lee – Department of Chemistry and Nano Science, Ewha Womans University, Seoul 03760, Korea;

orcid.org/0000-0002-5553-1453

Mian Guo – Department of Chemistry and Nano Science, Ewha Womans University, Seoul 03760, Korea;

orcid.org/0000-0001-7460-5852

Shunichi Fukuzumi – Department of Chemistry and Nano Science, Ewha Womans University, Seoul 03760, Korea;

orcid.org/0000-0002-3559-4107

Complete contact information is available at:

<https://pubs.acs.org/doi/10.1021/jacs.0c10159>

Notes

The authors declare no competing financial interest.

■ ACKNOWLEDGMENTS

This work was supported by the NRF of Korea through CRI (NRF-2012R1A3A2048842).

■ REFERENCES

- (1) (a) Larson, V. A.; Battistella, B.; Ray, K.; Lehnert, N.; Nam, W. Iron and Manganese Oxo Complexes, Oxo Wall and Beyond. *Nat. Rev. Chem.* **2020**, *4*, 404–419. (b) Guo, M.; Corona, T.; Ray, K.; Nam, W. Heme and Nonheme High-Valent Iron and Manganese Oxo Cores in Biological and Abiological Oxidation Reactions. *ACS Cent. Sci.* **2019**, *5*, 13–28. (c) Sahu, S.; Goldberg, D. P. Activation of Dioxxygen by Iron and Manganese Complexes: A Heme and Nonheme Perspective. *J. Am. Chem. Soc.* **2016**, *138*, 11410–11428.
- (2) (a) Dubey, K. D.; Shaik, S. Cytochrome P450 - the Wonderful Nanomachine Revealed through Dynamic Simulations of the Catalytic Cycle. *Acc. Chem. Res.* **2019**, *52*, 389–399. (b) Moody, P. C. E.; Raven, E. L. The Nature and Reactivity of Ferryl Heme in Compounds I and II. *Acc. Chem. Res.* **2018**, *51*, 427–435. (c) Guengerich, F. P. Mechanisms of Cytochrome P450-Catalyzed Oxidations. *ACS Catal.* **2018**, *8*, 10964–10976. (d) Huang, X.; Groves, J. T. Oxygen Activation and Radical Transformations in Heme Proteins and Metalloporphyrins. *Chem. Rev.* **2018**, *118*, 2491–2553. (e) Baglia, R. A.; Zaragoza, J. P. T.; Goldberg, D. P. Biomimetic Reactivity of Oxygen-Derived Manganese and Iron Porphyrinoid Complexes. *Chem. Rev.* **2017**, *117*, 13320–13352. (f) Yosca, T. H.; Ledray, A. P.; Ngo, J.; Green, M. T. A New Look at the Role of Thiolate Ligation In Cytochrome P450. *J. Biol. Inorg. Chem.* **2017**, *22*, 209–220.
- (3) (a) Banerjee, R.; Jones, J. C.; Lipscomb, J. D. Soluble Methane Monooxygenase. *Annu. Rev. Biochem.* **2019**, *88*, 409–431. (b) Kal, S.; Que, L. Dioxxygen Activation by Nonheme Iron Enzymes with the 2-His-1-Carboxylate Facial Triad that Generate High-Valent Oxoiron Oxidants. *J. Biol. Inorg. Chem.* **2017**, *22*, 339–365. (c) Solomon, E. I.; Goudarzi, S.; Sutherland, K. D. O₂ Activation by Non-Heme Iron Enzymes. *Biochemistry* **2016**, *55*, 6363–6374.
- (4) (a) Kal, S.; Xu, S.; Que, L., Jr Bio-inspired Nonheme Iron Oxidation Catalysis: Involvement of Oxoiron(V) Oxidants in Cleaving Strong C-H Bonds. *Angew. Chem., Int. Ed.* **2020**, *59*,

7332–7349. (b) Dantignana, V.; Company, A.; Costas, M. Oxoiron(V) Complexes of Relevance in Oxidation Catalysis of Organic Substrates. *Isr. J. Chem.* **2020**, *60*, 1–16. (c) Liu, Y.; Lau, T. C. Activation of Metal Oxo and Nitrido Complexes by Lewis Acids. *J. Am. Chem. Soc.* **2019**, *141*, 3755–3766. (d) Hong, S.; Lee, Y. M.; Ray, K.; Nam, W. Dioxygen Activation Chemistry by Synthetic Mononuclear Nonheme Iron, Copper and Chromium Complexes. *Coord. Chem. Rev.* **2017**, *334*, 25–42. (e) Engelmann, X.; Montepérez, I.; Ray, K. Oxidation Reactions with Bioinspired Mononuclear Non-Heme Metal-Oxo Complexes. *Angew. Chem., Int. Ed.* **2016**, *55*, 7632–7649. (f) Cook, S. A.; Borovik, A. S. Molecular Designs for Controlling the Local Environments around Metal Ions. *Acc. Chem. Res.* **2015**, *48*, 2407–2414. (g) Nam, W. Synthetic Mononuclear Nonheme Iron-Oxygen Intermediates. *Acc. Chem. Res.* **2015**, *48*, 2415–2423. (h) Puri, M.; Que, L., Jr Toward the Synthesis of More Reactive S = 2 Non-Heme Oxoiron(IV) Complexes. *Acc. Chem. Res.* **2015**, *48*, 2443–2452. (i) Nam, W.; Lee, Y. M.; Fukuzumi, S. Tuning Reactivity and Mechanism in Oxidation Reactions by Mononuclear Nonheme Iron(IV)-Oxo Complexes. *Acc. Chem. Res.* **2014**, *47*, 1146–1154. (j) Ray, K.; Pfaff, F. F.; Wang, B.; Nam, W. Status of Reactive Non-Heme Metal-Oxygen Intermediates in Chemical and Enzymatic Reactions. *J. Am. Chem. Soc.* **2014**, *136*, 13942–13958.

(5) Yoshimura, A.; Zhdankin, V. V. Advances in Synthetic Applications of Hypervalent Iodine Compounds. *Chem. Rev.* **2016**, *116*, 3328–3435.

(6) Nam, W. Dioxygen Activation by Metalloenzymes and Models. *Acc. Chem. Res.* **2007**, *40*, 465 and references therein.

(7) (a) Nam, W.; Ryu, Y. O.; Song, W. J. Oxidizing Intermediates in Cytochrome P450 Model Reactions. *J. Biol. Inorg. Chem.* **2004**, *9*, 654–660. (b) Collman, J. P.; Chien, A. S.; Eberspacher, T. A.; Brauman, J. I. Multiple Active Oxidants in Cytochrome P-450 Model Oxidations. *J. Am. Chem. Soc.* **2000**, *122*, 11098–11100. (c) Newcomb, M.; Hollenberg, P. F.; Coon, M. J. Multiple Mechanisms and Multiple Oxidants in P450-Catalyzed Hydroxylations. *Arch. Biochem. Biophys.* **2003**, *409*, 72–79. (d) Bryliakov, K. P.; Talsi, E. P. Evidence for the Formation of an Iodosylbenzene(salen)iron Active Intermediate in a (Salen)iron(III)-Catalyzed Asymmetric Sulfide Oxidation. *Angew. Chem., Int. Ed.* **2004**, *43*, 5228–5230. (e) Wang, S. H.; Mandimutsira, B. S.; Todd, R.; Ramdhanie, B.; Fox, J. P.; Goldberg, D. P. Catalytic Sulfoxidation and Epoxidation with a Mn(III) Triazacorrole: Evidence for A “Third Oxidant” in High-Valent Porphyrinoid Oxidations. *J. Am. Chem. Soc.* **2004**, *126*, 18–19. (f) Collman, J. P.; Zeng, L.; Wang, H. J. H.; Lei, A.; Brauman, J. I. Kinetics of (Porphyrin)manganese(III)-Catalyzed Olefin Epoxidation with a Soluble Iodosylbenzene Derivative. *Eur. J. Org. Chem.* **2006**, *2006*, 2707–2714.

(8) Guo, M.; Lee, Y. M.; Seo, M. S.; Kwon, Y. J.; Li, X. X.; Ohta, T.; Kim, W. S.; Sarangi, R.; Fukuzumi, S.; Nam, W. Mn(III)-Iodosylarene Porphyrins as an Active Oxidant in Oxidation Reactions: Synthesis, Characterization, and Reactivity Studies. *Inorg. Chem.* **2018**, *57*, 10232–10240.

(9) (a) Jeong, D.; Ohta, T.; Cho, J. Structure and Reactivity of a Mononuclear Nonheme Manganese(III)-Iodosylarene Complex. *J. Am. Chem. Soc.* **2018**, *140*, 16037–16041. (b) Hill, E. A.; Kelty, M. L.; Filatov, A. S.; Anderson, J. S. Isolable Iodosylarene and Iodoxyarene Adducts of Co and Their O-atom Transfer and C-H Bond Activation Reactivity. *Chem. Sci.* **2018**, *9*, 4493–4499. (c) de Ruiter, G.; Carsch, K. M.; Gul, S.; Chatterjee, R.; Thompson, N. B.; Takase, M. K.; Yano, J.; Agapie, T. Accelerated Oxygen Atom Transfer and C-H Bond Oxygenation by Remote Redox Changes in Fe₃Mn-Iodosobenzene Adducts. *Angew. Chem., Int. Ed.* **2017**, *56*, 4772–4776. (d) Au-Yeung, K. C.; So, Y. M.; Wang, G. C.; Sung, H. H. Y.; Williams, I. D.; Leung, W. H. Iodosylbenzene and Iodolbenzene Adducts of Cerium(IV) Complexes Bearing Chelating Oxygen Ligands. *Dalton Trans.* **2016**, *45*, 5434–5438. (e) de Sousa, D. P.; Wegeberg, C.; Vad, M. S.; Mørup, S.; Frandsen, C.; Donald, W. A.; McKenzie, C. J. Halogen-Bonding-Assisted Iodosylbenzene Activation by a Homogenous Iron Catalyst. *Chem. - Eur. J.* **2016**, *22*, 3810–3820. (f) Wang, C.; Kurahashi, T.; Inomata, K.; Hada, M.; Fujii, H. Oxygen-Atom

Transfer from Iodosylarene Adducts of a Manganese(IV) Salen Complex: Effect of Arenes and Anions on I(III) of the Coordinated Iodosylarene. *Inorg. Chem.* **2013**, *52*, 9557–9566. (g) Lennartson, A.; McKenzie, C. J. An Iron(III) Iodosylbenzene Complex: A Masked Non-Heme Fe^{IV}O. *Angew. Chem., Int. Ed.* **2012**, *51*, 6767–6770. (h) Wang, C.; Kurahashi, T.; Fujii, H. Structure and Reactivity of an Iodosylarene Adduct of a Manganese(IV)-Salen Complex. *Angew. Chem., Int. Ed.* **2012**, *51*, 7809–7811. (i) Smegal, J. A.; Hill, C. L. Synthesis, Characterization, and Reaction Chemistry of a Bis-(iodosylbenzene)-Metalloporphyrin Complex, [PhI(OAc)-O]₂Mn^{IV}TPP. A Complex Possessing a Five-Electron Oxidation Capability. *J. Am. Chem. Soc.* **1983**, *105*, 2920–2922.

(10) (a) Yang, J.; Seo, M. S.; Kim, K. H.; Lee, Y. M.; Fukuzumi, S.; Shearer, J.; Nam, W. Structure and Unprecedented Reactivity of a Mononuclear Nonheme Cobalt(III) Iodosylbenzene Complex. *Angew. Chem., Int. Ed.* **2020**, *59*, 13581–13585. (b) Wang, B.; Lee, Y. M.; Seo, M. S.; Nam, W. Mononuclear Nonheme Iron(III)-Iodosylarene and High-Valent Iron-Oxo Complex in Olefin Epoxidation Reactions. *Angew. Chem., Int. Ed.* **2015**, *54*, 11740–11744. (c) Hong, S.; Wang, B.; Seo, M. S.; Lee, Y. M.; Kim, M. J.; Kim, H. R.; Ogura, T.; Garcia-Serres, R.; Clémancey, M.; Latour, J. M.; Nam, W. Highly Reactive Nonheme Iron(III) Iodosylarene Complexes in Alkane Hydroxylation and Sulfoxidation Reactions. *Angew. Chem., Int. Ed.* **2014**, *53*, 6388–6392. (d) Song, W. J.; Sun, Y. J.; Choi, S. K.; Nam, W. Mechanistic Insights into the Reversible Formation of Iodosylarene-Iron Porphyrin Complexes in Reactions of Oxoiron(IV) Porphyrin π -Cation Radicals and Iodoarenes: Equilibrium, Epoxidizing Intermediate, and Oxygen Exchange. *Chem. - Eur. J.* **2006**, *12*, 130–137. (e) Nam, W.; Choi, S. K.; Lim, M. H.; Rohde, J. U.; Kim, I.; Kim, J.; Kim, C.; Que, L., Jr Reversible Formation of Iodosylbenzene-Iron Porphyrin Intermediates in the Reaction of Oxoiron(IV) Porphyrin π -Cation Radicals and Iodobenzene. *Angew. Chem., Int. Ed.* **2003**, *42*, 109–111.

(11) Abbreviations used: TDCPP, *meso*-tetrakis(2,6-dichlorophenyl)porphinato dianion; TDFPP, *meso*-tetrakis(2,6-difluorophenyl)porphinato dianion; TPFPP, *meso*-tetrakis(2,3,4,5,6-pentafluorophenyl)porphinato dianion.

(12) Guo, M.; Seo, M. S.; Lee, Y. M.; Fukuzumi, S.; Nam, W. Highly Reactive Manganese(IV)-Oxo Porphyrins Showing Temperature-Dependent Reversed Electronic Effect in C-H Bond Activation Reactions. *J. Am. Chem. Soc.* **2019**, *141*, 12187–12191.

(13) Luo, Y. R. *Handbook of Bond Dissociation Energies in Organic Compounds*; CRC Press: Boca Raton, FL, 2003.

(14) Fujii, H. Electronic Structure and Reactivity of High-Valent Oxo Iron Porphyrins. *Coord. Chem. Rev.* **2002**, *226*, 51–60.

(15) Garcia-Bosch, I.; Company, A.; Cady, C. W.; Styling, S.; Browne, W. R.; Ribas, X.; Costas, M. Evidence for a Precursor Complex in C-H Hydrogen Atom Transfer Reactions Mediated by a Manganese(IV) Oxo Complex. *Angew. Chem., Int. Ed.* **2011**, *50*, 5648–5653.

(16) Neu, H. M.; Yang, T.; Baglia, R. A.; Yosca, T. H.; Green, M. T.; Quesne, M. G.; de Visser, S. P.; Goldberg, D. P. Oxygen-Atom Transfer Reactivity of Axially Ligated Mn(V)-Oxo Complexes: Evidence for Enhanced Electrophilic and Nucleophilic Pathways. *J. Am. Chem. Soc.* **2014**, *136*, 13845–13852.

(17) (a) Ishizuka, T.; Ohzu, S.; Kotani, H.; Shiota, Y.; Yoshizawa, K.; Kojima, T. Hydrogen Atom Abstraction Reactions Independent of C-H Bond Dissociation Energies of Organic Substrates in Water: Significance of Oxidant-Substrate Adduct Formation. *Chem. Sci.* **2014**, *5*, 1429–1436. (b) Kojima, T.; Hirai, Y.; Ishizuka, T.; Shiota, Y.; Yoshizawa, K.; Ikemura, K.; Ogura, T.; Fukuzumi, S. A Low-Spin Ruthenium(IV)-Oxo Complex: Does the Spin State Have an Impact on the Reactivity? *Angew. Chem., Int. Ed.* **2010**, *49*, 8449–8453. (c) Park, J.; Lee, Y.-M.; Nam, W.; Fukuzumi, S. Brønsted Acid-Promoted C-H Bond Cleavage via Electron Transfer from Toluene Derivatives to a Protonated Nonheme Iron(IV)-Oxo Complex with No Kinetic Isotope Effect. *J. Am. Chem. Soc.* **2013**, *135*, 5052–5061.

(18) (a) Mayer, J. M. Understanding Hydrogen Atom Transfer: From Bond Strengths to Marcus Theory. *Acc. Chem. Res.* **2011**, *44*,

36–46. (b) Mader, E. A.; Mayer, J. M. The Importance of Precursor and Successor Complex Formation in a Bimolecular Proton-Electron Transfer Reaction. *Inorg. Chem.* **2010**, *49*, 3685–3687.

(19) Kang, Y.; Li, X. X.; Cho, K. B.; Sun, W.; Xia, C.; Nam, W. Mutable Properties of Nonheme Iron(III)-Iodosylarene Complexes Result in the Elusive Multiple-Oxidant Mechanism. *J. Am. Chem. Soc.* **2017**, *139*, 7444–7447.

(20) (a) Neu, H. M.; Baglia, R. A.; Goldberg, D. P. A Balancing Act: Stability versus Reactivity of Mn(O) Complexes. *Acc. Chem. Res.* **2015**, *48*, 2754–2764. (b) Li, X. X.; Guo, M.; Cho, K. B.; Sun, W.; Nam, W. High-Spin Mn(V)-Oxo Intermediate in Nonheme Manganese Complex-Catalyzed Alkane Hydroxylation Reaction: Experimental and Theoretical Approach. *Inorg. Chem.* **2019**, *58*, 14842–14852. (c) Hong, S.; Lee, Y. M.; Sankaralingam, M.; Vardhaman, A. K.; Park, Y. J.; Cho, K. B.; Ogura, T.; Sarangi, R.; Fukuzumi, S.; Nam, W. A Manganese(V)-Oxo Complex: Synthesis by Dioxygen Activation and Enhancement of Its Oxidizing Power by Binding Scandium Ion. *J. Am. Chem. Soc.* **2016**, *138*, 8523–8532. (d) Yang, T.; Quesne, M. G.; Neu, H. M.; Reinhard, F. G. C.; Goldberg, D. P.; de Visser, S. P. Singlet versus Triplet Reactivity in an Mn(V)-Oxo Species: Testing Theoretical Predictions Against Experimental Evidence. *J. Am. Chem. Soc.* **2016**, *138*, 12375–12386.

(21) Although it is less likely, we cannot exclude a high-spin $S = 1$ Mn(V)-oxo porphyrin species with no axial ligand trans to the Mn–O moiety as a possible intermediate, since this Mn(V)–O species has not been captured and/or synthesized yet.